Silicone Rubber Thermal Interface Materials: Applications and Performance Considerations

David C. Timpe Jr.
Arlon – Silicone Technologies Division
1100 Governor Lea Road, Bear, DE 19701
P: 800-635-9333 F: 302-834-2100 E: dtimpe@arlon-std.com

Abstract

Simple composits of silicone rubber, extending filler, and fiberglass offer an attractive combination of thermal, physical, and electric properties that make these materials an ideal choice for use as thermal interface materials. Good dielectric strength and low thermal impedance that is relatively stable from 8 to 200 psi of pressure offer excellent performance in pad applications such as transistor to heatsink mounting. The addition of high shear strength and low shear modulus offer excellent performance in adhesive applications such as photovoltaic to heatsink mounting where performance is demanded for 30 years or more. Transistor and photovoltaic applications are discussed and two new silicone thermal interface materials for use as pad or adhesives are present and compared to current offsets.

Keywords: polydimethylsiloxane (PDMS), silicone, thermal interface material (TIM), thermal conductivity, thermal impedance

Introduction

Controlling temperature in electronic assemblies is critical to semiconductor performance and life expectancy. The temperature may be largely generated internally during operation as in the case of transistors or externally from the environment as in the case of photovoltaic cells. Regardless the source, in most cases it is advantageous to remove as much heat as possible by dissipation from the assembly with the goal of lower operating temperature and reduced variability during operation. The design engineer has many options to achieve this goal but the most common is dissipation via heatsink [1, 2, 3]. The most common heatsink is a stamped or extruded aluminum part that accepts heat from an attached component and transfers it to the environment [1].

Application Examples

A transistor is a solid state switch that is controlled by an electric current. When power is applied to one lead of the transistor the semiconductor allows power to flow through the junction. This flow of power causes a rise in temperature at the junction. According to Pshaenich, the reliability, life expectancy, and performance of a semiconductor is a direct function of the junction temperature. Generally, for every 10°C above 100°C the operational life of the semiconductor is halved [4]. This means that thermal management of the junction temperature is critical to the performance of the semiconductor and the entire electronic assembly.

A photovoltaic (PV) cell is a semiconductor capable of converting sunlight into electricity. The semiconductor can be constructed from various materials including crystalline silicon or conjugated polymers [7, 8]. As the PV absorbs light from the sun and converts it into electricity it also absorbs heat that results in a temperature rise. Van Dyk et al. found that the effect of temperature on power produced degrades linearly at 0.23 W/^{o}C from 25°C to 70°C for a mono-crystalline silicon PV [7]. This is a 20% reduction in produced power due to thermal build up. Other studies have identified a 0.5% efficiency loss per ^{o}C. This equates to a 22.5% reduction in produced power in the assembly used by Van Dyk et al. [8]. Zauscher referenced a study by Notter et al. showing the average efficiency of a PV array was actually higher in the winter months due to lower temperatures but total electrical power produced remained higher in the summer due to longer duration of solar irradiance [9]. This suggests that thermal management of the PV cell is critical to the performance of the semiconductor and assembly particularly when the assembly is used in areas with high ambient temperatures.

Figure 1 shows a side view of a TO-220 transistor mechanically attached to a heatsink. The metal tab of the transistor is almost always electrically active so it must be isolated from the heatsink to prevent the

heatsink from being electrically active inside the enclosure [1]. This is accomplished by placing an electrically insulating thermal interface material (TIM) between the transistor and heatsink. The TIM can adhesively bond the transistor to the heatsink or it may be mechanically attached with a screw or clip. Ideally, the TIM should not only electrically isolate the transistor but should also have low thermal resistance so heat is efficiently conducted from the transistor to the heatsink. When mechanical attachment is used, the TIM should also be highly conformable so pressure is uniformly distributed across the area akin to a press pad [5]. When bonding is required the TIM should have high shear strength and a low shear modulus. The high shear strength and low shear modulus allow for the decoupling of stress induced by differences in the coefficient of thermal expansion (CTE) at a minimum of thickness [6].

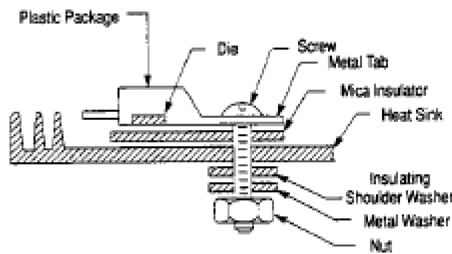

Figure 1 – Side view of a transistor/heatsink [4].

Materials

Effectively removing heat from a component or assembly is highly dependent on the identification and selection of the appropriate TIM. In many cases the TIM must electrically isolate the heatsink, have low thermal impedance, and in the case of pads be highly conformable. The TIM must also have high shear strength and low shear modulus when operating as an adhesive system. TIM pads and adhesives based on simple composites of silicone rubber, extending filler, and fiberglass fabric are capable of delivering excellent performance in these areas.

Two TIM's from Arlon and a leading competitor consisting of silicone rubber, an extending filler system, and a fiberglass support fabric, were evaluated comparatively for thermal impedance as a function of pressure, shear strength, shear modulus, and dielectric breakdown strength. Each TIM can be used in the uncured state as an adhesive system or in the cured state as a pad.

The apparent thermal conductivity of each TIM was measured by ASTM D5470 test method [10]. The method uses a one dimensional, steady state, heat flow to determining thermal transmission properties of sheet materials and is well suited and accepted for use with these types of materials. Fixture pressure was 435 +/- 15 psi and average sample temperature was 50 +/- 1°C. The apparent thermal conductivity results are compared to published values for competitive materials (Figure 2). The apparent thermal conductivity of Arlon A is within 10% of Competitor A and Arlon B is within 10% of Competitor B. All materials have a target thickness of 0.009 inches.

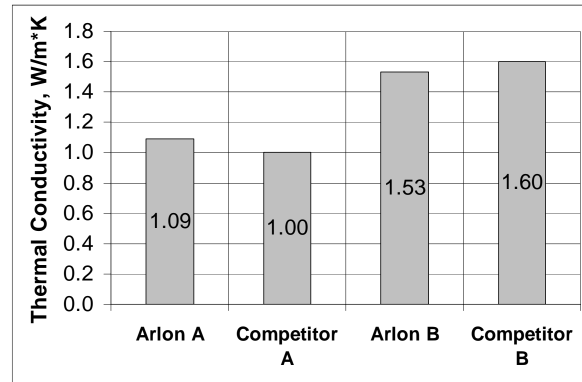

Figure 2 – Apparent thermal conductivity of Arlon A and B TIM by ASTM D5470 and published datasheet values for Competitor A and B TIM.

The thermal impedance of each TIM as a function of pressure was measured using the ASTM D5470 fixture. Fixture pressures from 8 to 200 PSI were evaluated. The average sample temperature was 50 +/- 2°C. The thermal impedance is the total thermal resistance which includes the thermal resistance of the TIM and the thermal contact resistance of the TIM in contact with the fixture. The thermal impedance therefore depends not only on the material but how well the surface of the material and the surface of the fixture mate. For this reason it is expected that different test fixtures will produce different results and that the results measured in a specific test fixture may not translate for an actual application. However, it is reasonable to compare two materials in the same fixture under equivalent test condition which is what has been done in this experimental analysis.

Figure 3 shows the effect of pressure on thermal impedance of Arlon A and Competitor A. The thermal impedance of both products follows a power function. It can be seen that both materials have similar thermal impedance at 200 psi, but the effect of decreasing pressure is more significant for Competitor A than Arlon A. One potential cause for this is the difference in surface topography of the two materials. Arlon A is significantly smoother than Competitor A (Image 1 and 2). The large irregularly shaped

particles as well as the topography caused by the supporting fabric or coating method can clearly be seen in Competitor A.

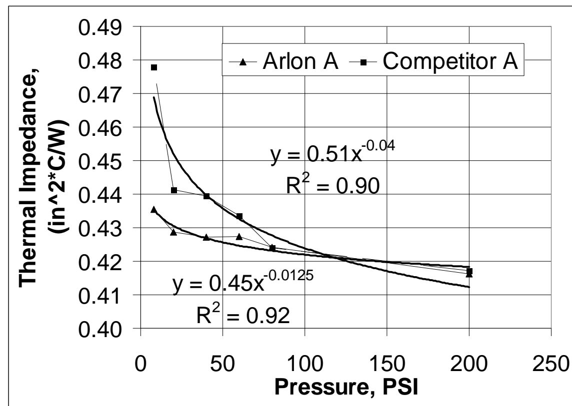

Figure 3 – Thermal impedance as a function of pressure for Arlon A and Competitor A.

Image 1 – Arlon A micrograph. Area is 0.008 in^2

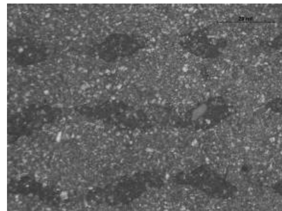

Image 2 – Competitor A micrograph. Area is 0.008 in^2.

Figure 4 shows the effect of pressure on thermal impedance of Arlon B and Competitor B. The thermal impedance of both products follows a power function. It can be seen that the thermal impedance of Competitor B is approximately 10% higher than Arlon B at 200 psi. The disparity in thermal impedance between the two products continues as the pressure is decreased. The potential cause is again the surface topography. The topography of Arlon B is smooth (Image 3). No extending filler particles are visible in the Competitor B sample, but the topography caused by the supporting fabric and coating method is even more pronounced (Image 4). The lighter areas of the Competitor B micrograph account for approximately 45% of the total area. These areas correlate to the peaks of the supporting fiberglass and at low pressure are likely the only areas of the material making contact with the test fixture. Poor mating is most likely the cause of higher thermal impedance and greater dependence on pressure.

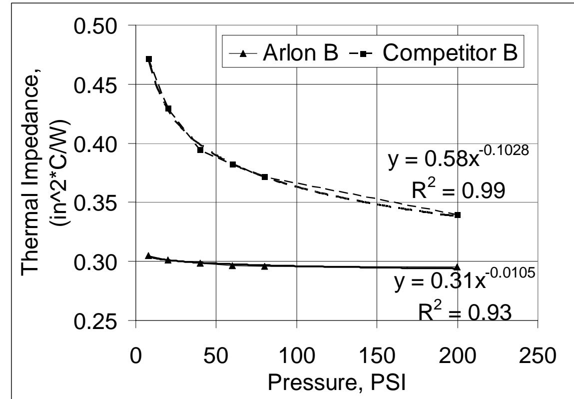

Figure 4 – Thermal impedance as a function of pressure for Arlon B and Competitor B.

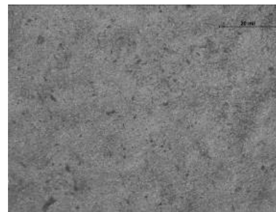

Image 3 – Arlon B micrograph. Area is 0.008 in^2.

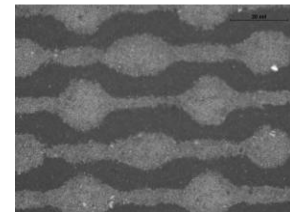

Image 4 – Competitor B micrograph. Area is 0.008 in^2.

The lap shear strength of Arlon A and B was evaluated per ASTM D1002 (Figure 5) [11]. Lap shear coupons were assembled using 6 in. x 1 in. x 0.063 in. T-6061 aluminum coupons adhered with 1 in^2 of material in a single-lap-joint configuration. Coupons were press cured in a hydraulic platen press for 15 minutes at 121°C. No additional time was provided to account for thermal lag of tooling. Coupons were tested for shear strength and shear modulus in an Instrumet 1120 tensile testing machine with a 1,000 lb. load cell and a crosshead speed of 0.014 inches/minute. The shear strength of Arlon A and B is given in Figure 5. Lap shear testing of Competitor A and B is not possible because they are only available in the cured form for use as pads.

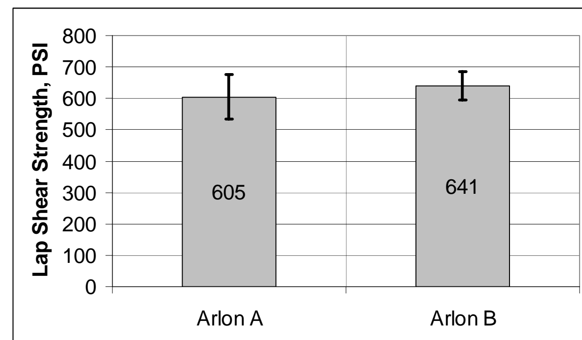

Figure 5 – Lap shear strength of Arlon A and B. Error bars represent 3 standard deviations.

Shear modulus was determined from the stress stain curves generated during lap shear testing on Arlon A and B by linear regression in the entire strain range, which exceeded 500% percent. The regression line slope is the shear modulus (Figure 6) with correlation coefficients (R^2) exceeding 0.99. Shear modulus determination of Competitor A and B was also not determined.

The shear modulus of Arlon A and B is given in Figure 6.

Figure 6 – Shear modulus of Arlon A and B

The dielectric strength of Arlon A and B was evaluated per ASTM D149 (Figure 7) [12]. Samples were tested with 60 Hz AC current with a 0.25 in. diameter electrode.

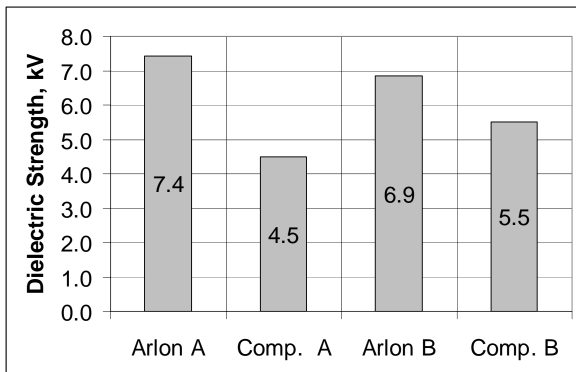

Figure 7 – Dielectric Strength of 0.009" thick Arlon A and B per ASTM D149 and published datasheet values for 0.009" thick Competitor A and B.

Conclusion:

The Arlon A and B TIM's offer excellent thermal, mechanical, and electrical properties. As pads their low surface topography and conformability results in low thermal impedance. As adhesives they provide the added benefit, in addition to low thermal impedance, of stress decoupling over a wide range of operation temperatures due to their high shear strength and low shear modulus. As both adhesives and pads they provide good electrical isolation with high AC dielectric breakdown strength.

References

[1] Balog, R. (2003, April 7). How to keep your cool while working with power electronics: static thermal design issues. Retrieved June 9, 2010, from http://www.ece.tamu.edu/~rbalog/publications/How%20to%20keep%20your%20cool%20when%20working%20with%20power%20electronics.pdf

[2] Poech, M. H., & Ahrens, T. (n.d.). Heat dissipation. Retrieved June 9, 2010, from http://thermal.electronics-ktn.com/thermal/webcasts/storyboards/ahrens08.pdf

[3] Srinivasan, J., Adve, S. V., Bose, P., & Rivers, J. A. (2004, June). The impact of technology scaling on lifetime reliability. The International Conference on Dependable Systems and Networks. Retrieved from http://citeseerx.ist.psu.edu/viewdoc/download?doi=10.1.1.5.8306&rep=rep1&type=pdf

[4] Pshaenich, A. (1990). Basic thermal management of power semiconductors. Retrieved June 9, 2010

[5] Zhang, H., Cloud, A., Timpe, D. C., & Amalfitano, G. (2008, April 28). Low cost per cycle silicone press pad with predictable service life. Retrieved June 9, 2010, from http://www.arlon-std.com/Library/Guides/UltraPad_04282008.pdf

[6] Zhang, H. (2005, December 12). Thermal-mechanical decoupling by a thermal interface material. Retrieved June 9, 2010, from http://www.arlon-std.com/Library/Guides/Thermal%20Mechanical%20Decoupling%20by%20a%20TIM.pdf

[7] Van Dyk, E., Meyer, E., Leitch, A., & Scott, B. (2000). Temperature dependence of performance of crystalline silicon photovoltaic modules. South African Journal of Science, 96(4), 198-200. Retrieved from Academic Search Premier database.

[8] Schuller, S., Schilinsky, P., Hauch, J., & Brabec, C. (2004). Determination of the degradation constant of bulk heterojunction solar cells by accelerated lifetime measurements. Applied Physics A, 79, 37-40. doi:10.1007/s00339-003-2499-4

[9] Zauscher, M. D. (2006, December 7). Solar photovoltaic panels from a heat transfer perspective.

Retrieved June 9, 2010, from http://courses.ucsd.edu/rherz/mae221a/reports/Zauscher_221A_F06.pdf

[10] “Standard Test Method for Thermal Transmission Properties of Thin Thermally Conductive Solid Electrical Insulation Materials”, ASTM D5470, ASTM International, West Conshohocken, PA, 2004.

[11] “Standard Test Method for Apparent Shear Strength of Single-Lap-Joint Adhesively Bonded Metal Specimens by Tension Loading (Metal-to-Metal)”, ASTM D1002, ASTM International, West Conshohocken, PA, 2004.

[12] “Standard Test Method for Dielectric Breakdown Voltage and Dielectric Strength of Solid Electrical Insulating Materials at Commercial Power Frequencies”, ASTM D149, ASTM International, West Conshohocken, PA, 2004.